Comparing Geometries for Magnetic Bearings

D. F. B. DAVID*, J. A. SANTISTEBAN* and A. C. DEL NERO GOMES**
* Universidade Federal Fluminense
Rua Passo da Pátria 156, 24210-240, Niteroi, Brasil
** Universidade Federal do Rio de Janeiro
CP 68504, 21945-070, Rio de Janeiro, Brasil

Abstract
Most Active Magnetic Bearings (AMBs) show a symmetry of 4 geometry, because the magnetic forces are generated in 4 points in a plane, two in the canonical x direction and two in the y direction. AMBs with symmetry of 3 are harder to find, either in real-world applications or in the specific literature. Their stators generate forces in 3 coplanar points; one of these, at most, can lie in one of the canonical x, y directions. This work will develop and analyse mathematical models for the symmetry of 3 AMBs; in some cases these models can be problematic. Some comparisons will also be made between these two basic geometries trying to decide whether one or the other should be used in practical applications.

Keywords : Symmetry of 4, Symmetry of 3, Uncoupled fluxes, Coupled fluxes, AMBs geometry

1. Introduction

The majority of Active Magnetic Bearings (AMBs), either in real-world applications or mentioned in the literature, show the structure on the left side of Figure 1. The four U-shaped electromagnets generate restoring forces in the x and y directions; the windings are rigged in a way that results in four independent magnetic flux loops [1,3,10].This geometry is characterized by eight poles, or stubs or teeth leaving the stator and pointing inwards to form the eight gaps separating the stator and rotor. This structure can be refered to as 8 gaps, 8 poles, or uncoupled fluxes (UF).

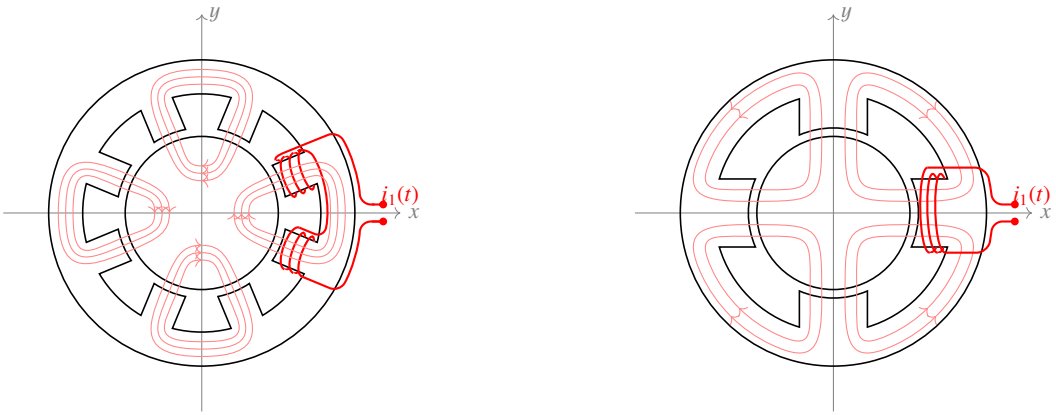

Fig. 1 Windings are shown for the positive x direction only; opposing pairs of windings along the $x(y)$ direction control that position. In the traditional AMB, at the left, there are no connections among the flux paths; in the four-pole case, at the right, the flux paths are interconnected.

There are other possible types of AMBs [4,5,6,7].The right side of Figure 1 depicts a structure that mixes the fluxes in the rotor and can be called 4 gaps, 4 poles, or coupled fluxes (CF). In both cases, the windings in the x, y directions are fed with currents $i_i = i_0 \pm i_{x,y}(t)$; the differential currents $i_{x,y}$ will control the rotor position [3,10,11].The resultant forces $f_{x,y}$ can be expressed in terms of these currents, the air magnetic permeability μ_0, the number of coils n, the cross-section areas A and the nominal length h of the air gaps

The previous geometries exhibit symmetry of 4 (Sym4), because the forces are generated in 4 points. AMBs with 06 or 03 poles are harder to find in applications or in the literature [1,2,8,9,12].Their stators show symmetry of 3 (Sym3); a basic picture of the situation is shown in Figure 2. In the 6 gaps each pair of poles performs as a U-shaped electromagnet. All the flux injected in the rotor by one of the poles is absorbed by the adjacent pole; the fluxes generated by one of the electromagnets do not intercept the fluxes from the other channels and this explains the name uncoupled or unconnected Fluxes (UF). In the 3 gaps, the situation changes completely, leading to coupled, mixed, connected fluxes (CF).

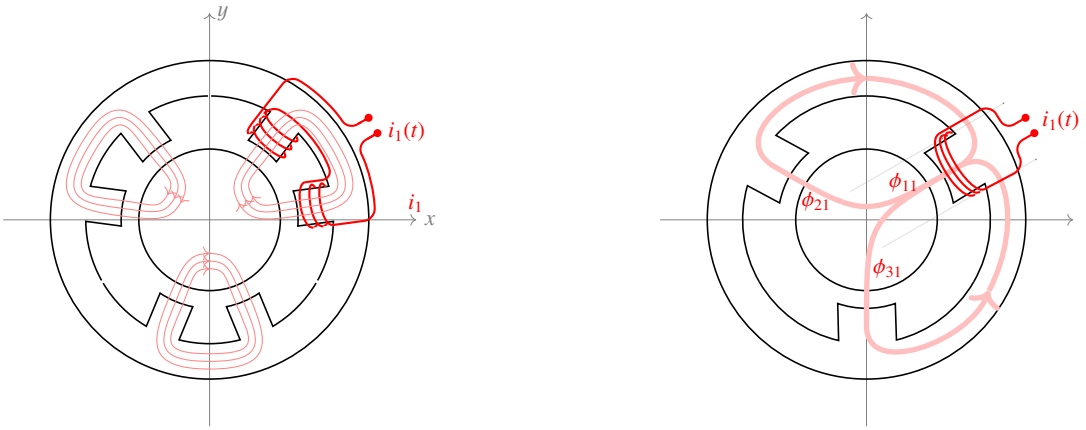

Fig. 2 Sym3 possibilities for AMBs: 6 gaps or 6 poles or UF (uncoupled fluxes) at the left and 3 gaps or 3 poles or CF (coupled fluxes) at the right. All windings control the x and y positions; only the current in direction 1 is shown.

The same aspects concerning the fluxes happen in the Sym4 world and many comparisons between the two resulting AMB structures can be found in [7].It is just natural to assume that a similar comparisons can be made in the Sym3 world. The work in [1].brings unexpected facts: the mathematical model for one possible CF geometry with 3 gaps cannot be linearized. Many possible geometries can provide CF in the Sym3 world and one of the goals of this paper is to study them, and also to compare the well-behaved UF geometries of 08 and 06 gaps to decide wether Sym3 AMBs are (or are not) possible alternatives to Sym4 devices.

2. Symmetry of 3 basic facts

More details about the following facts can be found in [1,9].Magnetic Devices (MDs) transform electric currents in forces; the side figure depicts 03 MDs symmetrically surrounding a particle. An easy way to represent MDs is used in this figure; in real life, most MDs are either cylindrically or U-shaped pieces of a ferromagnetic material surrounded by coils of wire.
The coordinates $x(t)$ and $y(t)$ (or the rotor position, in the AMBs case) are controlled by the forces $\boldsymbol{f}_k(t)$ for $k = 1, 2, 3$. The directions of these forces, see the side figure, can be considered fixed, for small displacements; projecting their absolute values in the x and y directions leads to

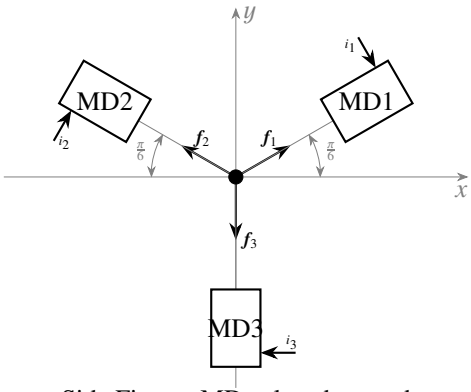

Side Figure: MDs placed around a centered particle

$$\sum_{k=1}^{3} f_k^x = f^x = (f_1 - f_2)\,\frac{\sqrt{3}}{2} \qquad \text{and} \qquad \sum_{k=1}^{3} f_k^y = f^y = (f_1 + f_2)\,\frac{1}{2} - f_3. \tag{1}$$

It is well known [3,10,11] that the reluctance forces produced in MDs depend on the square of the magnetic flux, the area occupied by it, and on the air magnetic permeability μ_0:

$$f_k(t) = \frac{\phi_k^2(t)}{\mu_0 A_k} \quad \text{for} \quad k = 1, 2, 3. \tag{2}$$

Each force depends only on the magnetic flux $\phi_k(t)$. In some cases, $\phi_k(t)$ is affected only by the current $i_k(t)$ and by the distance d_k between the body and MDk. This case is fairly easy to study but in other situations fluxes in each channel depend on the parameters of all MDs: $\phi_k(t) = \varphi_k\,(i_1(t), i_2(t), i_3(t), d_1(t), d_2(t), d_3(t))\ \ \forall k = 1, 2, 3$. The distance h between the origin and each actuator is fixed; let e_k measure the body's displacements, considered positive when pointing towards MDk. For significant load dimensions, as in AMBs, h is the nominal gap width. It is clear that

$$d_k(t) = h - e_k(t) \quad \text{for} \quad k = 1, 2, 3. \tag{3}$$

It is easier to measure the body's displacements $e_k(t)$ than its distances $d_k(t)$ to the MDs so the fluxes expression can be updated: $\phi_k(t) = \varphi_k\,(i_1(t), i_2(t), i_3(t), e_1(t), e_2(t), e_3(t))\ \ \forall k = 1, 2, 3$. The fluxes depend on 03 injected currents, and 03 displacements e_1, e_2, e_3. The e_k are redundant to determine the position in the plane, only two displacement sensors are installed in practical implementations, covering the canonical and orthogonal directions x and y. It is easy to see that, as shown in [1], the $e_k(t)$ are related to the measurable quantities $x(t)$ and $y(t)$ by

$$e_1(t) = \frac{\sqrt{3}x(t)}{2} + \frac{y(t)}{2} \quad \text{and} \quad e_2(t) = -\frac{\sqrt{3}x(t)}{2} + \frac{y(t)}{2} \quad \text{and} \quad e_3(t) = -y(t). \tag{4}$$

The $d_k = h - e_k$ with these values are approximations to the real distances between the body and the MDs. These numbers are small so this is accepted and used without any care. There are, now, only 05 variables affecting the fluxes in MDs and the previous equations can be further improved to $\phi_k(t) = \varphi_k\,(i_1(t), i_2(t), i_3(t), x(t), y(t))\ \ \forall k = 1, 2, 3$. To analyze if it is possible to position the particle with fewer than 3 control variables, particular cases will be considered.

3. AMBs with uncoupled fluxes

The next results can be found in [3,10,11]. An illustration of a Sym4 UF device is shown on the left side of figure 1. There are four pairs of poles in the stator; the word pole used here, and in all the paper, has no magnetic meaning, it indicates parts of the stator that point inwards. Each pair of poles performs as an independent U-shaped electromagnet. Simple facts on reluctance are used to find the force at each MD. Let μ_0 be the air magnetic permeability and the pole areas and the number of coils be equal to A and n. Using equation (2) for each pair of poles and (3): $f_k(t) = Ki_k(t)^2/(h - e_k(t))^2$ with $K = \mu_0 An^2/4$ for $k = 1, 2, 3, 4$. The forces on the rotor are $f^x = f_1 - f_3$ and $f^y = f_2 - f_4$. If x and y are the rotor displacements it is easy to see that $e_1 = x$, $e_2 = y$, $e_3 = -x$, and $e_4 = -y$. The result is

$$f^x = K\left[\left(\frac{i_1}{h - x}\right)^2 - \left(\frac{i_3}{h + x}\right)^2\right] \quad \text{and} \quad f^y = K\left[\left(\frac{i_2}{h - y}\right)^2 + \left(\frac{i_4}{h + y}\right)^2\right]. \tag{5}$$

The i_k currents depend on a fixed i_0 and two differential parts i_x and i_y: $i_{1,3} = i_0 \pm i_x$, $i_{2,4} = i_0 \pm i_y$. Using these allows a final form for the forces; they depend on x, y, i_x, i_y and can be linearized around the operating point $OP = (x^0, y^0, i_x^0, i_y^0) = (0, 0, 0, 0)$. The well-known result is

$$f^x = k_p x + k_i i_x \quad \text{and} \quad f^y = k_p y + k_i i_y \quad \text{where} \quad k_p = \frac{\mu_0 An^2 i_o^2}{h^3}, k_i = \frac{\mu_0 An^2 i_0}{h^2}. \tag{6}$$

The facts above consider Sym4 AMBs. More details about the following Sym3 results can be found in [1,9]. An illustration of a device is shown on the left side of figure 2. The fluxes ϕ_k are uncoupled, and basic results [3,10,11] are used to find the force at each MD. Assuming again equal areas and number of coils, equation (3) leads to $f_k(t) = Ki_k(t)^2/(h - e_k(t))^2$ with $K = \mu_0 An^2/4$ for $k = 1, 2, 3$. The forces on the rotor come from equation (1); the result is

$$f^x = \frac{K\sqrt{3}}{2}\left[\left(\frac{i_1}{d_1}\right)^2 - \left(\frac{i_2}{d_2}\right)^2\right] \quad \text{and} \quad f^y = \frac{K}{2}\left[\left(\frac{i_1}{d_1}\right)^2 + \left(\frac{i_2}{d_2}\right)^2 - 2\left(\frac{i_3}{d_3}\right)^2\right]. \tag{7}$$

Keeping in mind equation (4), and since $d_k = h - e_k$, the three distances in the above formulas depend on the displacements x and y only:

$$d_1 = h - \frac{\sqrt{3}}{2}x - \frac{1}{2}y; \qquad d_2 = h + \frac{\sqrt{3}}{2}x - \frac{1}{2}y; \qquad d_3 = h + y. \tag{8}$$

It is reasonable to consider a fixed base current i_0 and differential currents $v_k(t)$ to be rigged as

$$i_1(t) = i_0 + v_1(t); \qquad i_2(t) = i_0 + v_2(t); \qquad i_3(t) = i_0 + v_3(t). \tag{9}$$

A mathematical model for the force generation in 06 poles AMBs consists of equations (7), (8) and (9). The net result is $f^{xy} = g_{xy}(v_1, v_2, v_3, x, y)$. The linearization around the operating point OP $= (v_1^o, v_2^o, v_3^o, x^o, y^o) = (0, 0, 0, 0, 0)$ leads, after a thorough calculation, to

$$f^x = k_p x + \sqrt{3}k_v(v_1 - v_2),\ f^y = k_p y + k_v(v_1 + v_2 - 2v_3) \text{ where } k_p = \frac{3Ki_0^2}{h^3} \text{ and } k_v = \frac{Ki_0}{h^2}. \tag{10}$$

Using this expression in a linearized dynamic model for the AMB it can be seen that only two control currents i_x and i_y are needed to stabilize the system; one possible solution appears:

$$v_1 = -\frac{\sqrt{3}}{2}i_x - \frac{1}{2}i_y; \quad v_2 = \frac{\sqrt{3}}{2}i_x - \frac{1}{2}i_y; \quad v_3 = i_y. \tag{11}$$

This transforms (10) in a completely decoupled structurew; a nice and desired fact.

$$f^x = k_p x + k_i i_x, \quad f^y = k_p y + k_i i_y \quad \text{where} \quad k_p = 3\frac{\mu_0 A n^2 i_0^2}{4h^3} \quad \text{and} \quad k_i = -3\frac{\mu_0 A n^2 i_0}{4h^2} \tag{12}$$

3.1. Comparing Sym3 and Sym4

The forces in a UF Sym4 device are modelled by equations (5) and (6). For a UF Sym3 device equations (7) and (12) do the job. To compare these geometries, by simulations, a more complete AMB model is needed, taking into account the rotor dynamics. The simulations data come from a prototype [7] depicted in Figure 3. A vertical rotor fits in stators with different geometries. The upper disk generates harmonic disturbances that will not be considered here. The bottom part is a mechanical bearing to prevent vertical movements; above it comes the rotor of a motor for spinning the shaft and then the AMB rotor, the same for every geometry, and the sensors' target.

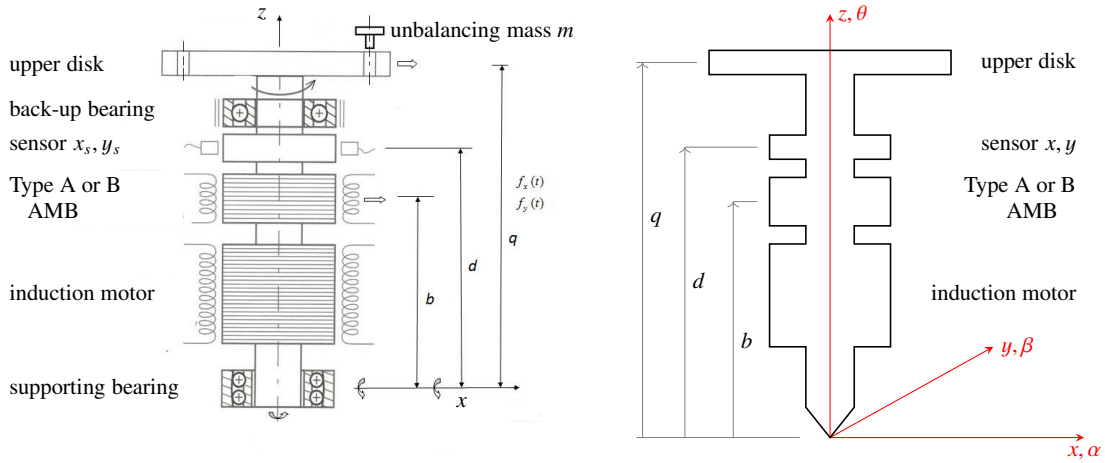

Fig. 3 Vertical rotor's aspects and dimensions, in the left part. In the right half, a simplified representation of its basic geometric aspects and dimensions.

Traditional methods [3,10,11] are used to model the rotor. The supporting bearing allows angular movements in any direction and provides a fixed point for the rotor. An inertial reference system is placed at this location; the positive angles α, β and θ are found with the right-hand rule on x, y and z. Assuming a rigid and homogeneous rotor, the center of mass displacements are determined by α and β, and a full model is obtained from the rotational equations alone. Denoting the angular moments of inertia by I_x, I_y and I_z, symmetry assures that $I_x = I_y = J$. In the classical Newton-Lagrange framework, the dynamic equations are:

$$J\ddot{\beta}(t) - \omega I_z\dot{\alpha}(t) = E_\beta \qquad \text{and} \qquad J\ddot{\alpha}(t) + \omega I_z\dot{\beta}(t) = E_\alpha \tag{13}$$

where $\omega = \dot{\theta}$ is the rotor angular velocity and $E_{\beta,\alpha}$ are the external torques that may come from different sources: magnetic, gravitational, supporting bearing and disturbance, or mass unbalance. Only magnetic and supporting bearing torques will be considered here. If x and y are the rotor displacements at the AMB position, then $\sin\beta = x/b$ and $\sin\alpha = -y/b$. The forces from the stator cause torques $P_\beta = bf^x\cos\beta$ and $P_\alpha = -bf^y\cos\alpha$. The supporting bearing has a viscous damper constant C_a generating torques $P_\beta = -C_a\dot{\beta}$ and $P_\alpha = -C_a\dot{\alpha}$. The model in (13) can be updated

$$J\ddot{\beta}(t) + C_a\dot{\beta}(t) = \omega I_z\dot{\alpha}(t) + f^x b\cos\beta \quad \text{and} \quad J\ddot{\alpha}(t) + C_a\dot{\alpha}(t) = -\omega I_z\dot{\beta}(t) - f^y b\cos\alpha \tag{14}$$

To relate the magnetic forces to the rotor linear displacements it suffices to remember that

$$x = b\sin\beta \qquad \text{and} \qquad y = -b\sin\alpha. \tag{15}$$

Equations (14) and (15) model the non-linear rotor motions. To linearize them recall that β and α are usually small, and for small x: $\sin x \approx x$ and $\cos x \approx 1$. Choosing $p_1 = \beta, p_2 = \alpha, p_3 = \dot{\beta}, p_4 = \dot{\alpha}$, a linear state space description is $\dot{\boldsymbol{p}}(t) = A_o\boldsymbol{p}(t) + B\boldsymbol{v}(t)$ where $\boldsymbol{p} = [p_1\ p_2\ p_3\ p_4]^T$, $\boldsymbol{v} = [f^x\ f^y]^T$. When the linearized f^x and f^y in (6) and (12) are used this equation changes to

$$\dot{\boldsymbol{p}}(t) = A\boldsymbol{p}(t) + B\boldsymbol{u}(t) \qquad \text{where} \qquad \boldsymbol{u} = [i_x\ i_y]^T. \tag{16}$$

A and B are 4×4 and 4×2 matrices respectfully structured as:

$$\begin{bmatrix} 0 & I_2 \\ A_{21} & A_{22} \end{bmatrix}, \begin{bmatrix} 0 \\ B_2 \end{bmatrix},\ A_{21} = \frac{b^2k_p}{J}I_2,\ A_{22} = \frac{1}{J}\begin{bmatrix} -C_a & \omega I_z \\ -\omega I_z & -C_a \end{bmatrix}, B_2 = \frac{bk_i}{J}\begin{bmatrix} 1 & 0 \\ 0 & -1 \end{bmatrix}. \tag{17}$$

It is important to notice that equation (16) models a linear system that is time invariant only for a fixed rotational speed, because A_{22} depends on ω.

3.2. Control

Choosing a control law for AMBs requires, in most cases, a linear model and so the linearized equations for each geometry will be used first. The LQR (Linear Quadratic Regulator), for which references abound, will be employed; it searches for $u(t)$ that minimizes the performance index

$$I_{xu} = \int_0^\infty \left(\boldsymbol{p}^T(t)Q\boldsymbol{p}(t) + \boldsymbol{u}^T(t)R\boldsymbol{u}(t)\right) \mathrm{d}t.$$

The solution is a state feedback $\boldsymbol{u} = F^*\boldsymbol{p}$ that drives the state to zero in an optimal way. Matrix Q emphasizes the importance of the state $\boldsymbol{p}$, while R is associated with the control cost, measured by the $\boldsymbol{u}$ curves. The values $Q = I_4$ and $R = I_2$ will be used in the simulations. Most softwares used in control applications, like Matlab and Octave, have simple commands to calculate F^*.

The first step of all simulations is to find the LQR F^* for the linear model (16); making $\boldsymbol{v} = F^*p$ means that i_x and i_y are expressed in terms of the state variables p_i. The next step is to use i_x and i_y in the non-linear models in (5) and (7); curves $x = b\sin\beta$ and $y = -b\sin\alpha$ can now be plotted. The prototypes characteristics were measured in the SI system; the geometric dimensions are $b = 0.137$, $d = 0.203$, $q = 0.252, r = 0.060$; the inertia and viscous values are $I_z = 0.0017, I_x = I_y = J = 0.0592, C_a = 0.0303$; the air gap is $h = 0.0005 = 5E-4$ and $\omega = 360$. A base current $i_0 = 1$ is considered and $K_0 = \mu_0 An^2 = 1.47725E5$; the magnetic coefficients $k_p =$ and k_i can be calculated for the both cases.

For the Sym4 case, the position and current constants are $k_p = K_0 i_0^2/h^3$ and $k_i = K_0 i_0/h^2$, with K_0 defined a few lines above. Octave was used and the result assigned the closed-loop eigenvalues to $-68.22 \pm j5.75$ and $-54.54 \pm j4.59$. The constants for Sym3 are $k_p = (3K_0/4)i_0^2/h^3$ and $k_i = -(3K_0/4)i_0/h^2$. The optimal solution, by Octave, assigns the closed-loop eigenvalues to $-58.14 \pm j5.67$ and $-47.88 \pm j4.67$. These solutions are in equation (18).

$$F_4^* = \begin{bmatrix} -544.1427 & 45.8247 & -8.9396 & 0.0000 \\ 45.8247 & 544.1427 & 0.0000 & 8.9396 \end{bmatrix} F_3^* = \begin{bmatrix} 542.8405 & -52.9319 & 10.2875 & 0.0000 \\ -52.9319 & -542.8405 & 0.0000 & -10.2875 \end{bmatrix} \tag{18}$$

In both cases, the differential currents i_x and i_y to be used in the linear model are given by $F^*\boldsymbol{p}$; for the non-linear model $F^*[\beta\ \alpha\ 't\beta\ \dot{\alpha}]^T$ must be used. For the initial conditions $x(0) = y(0) = h/(2b)$ the models of both devices were simulated in OpenModelica for 0.2s; the $x(t)$ and $y(t)$ curves are shown in Figure 4.

The convergence to the center is fast and with no overshoots in both cases. The differences between the two geometries are small and hard to detect in an open eye inspection. Even though Sym4 seems to be a little bit better, the differences are very small and affirming that, in the particular case of these simulations, both geometries perform in a very similar and interchangeable way must cause no fuss. Results for i_x and i_y, not shown here, behave in this very same way.

The curves are not presented here, but simulations for Sym4 and Sym3 with LQR controls calculated with [Q R[varying between [1024 1] and [1 1024] were made, with results very similar to the above ones. These simulations results are still in a shy beginning, but they allow us to say that, or hope for, Sym 3 and Sym4 UF devices are both valid attempts to use in AMBs.

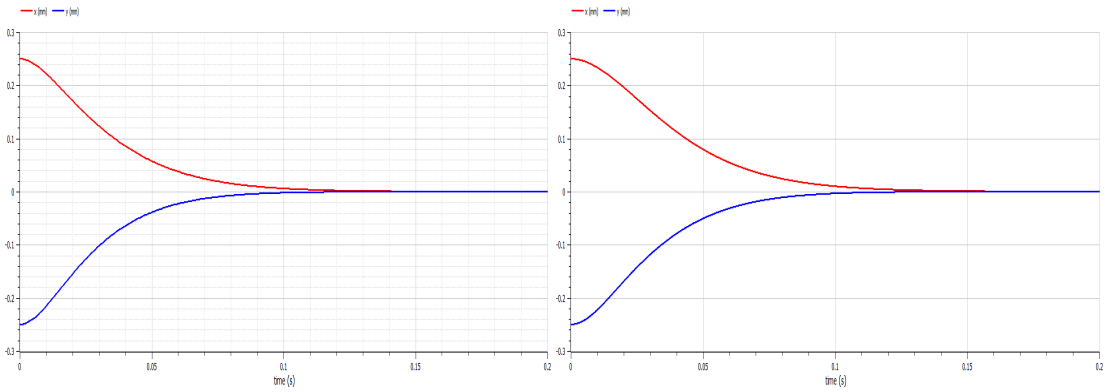

Fig. 4 Rotor displacements for a Sym4 AMB, at the left and a Sym3 at the right; red curves denote $x(t)$ and blue ones $y(t)$; the time span is 0.20s and the displacements range from ±0.3mm.

4. AMBs with coupled fluxes

Only the Sym3 case will be treated here; more details about the following results can be found in [1,9]. An illustration of a device is shown on the right side of figure 2. The mathematical model for this geometry, shown in [1] has a serious problem, its linearization is problematic. One of the main goals of this article is to investigate other coupled fluxes possibilities in the Sym3 world. The UF Sym3 covered in the last section is also called Type A, and the CF mentioned above is Type B. Type C geometry is represented in Figure 5: there are 03 flux injecting (for positive currents) poles and a neutral one that offers a simple exit or entrance for fluxes. Will this Sym3 geometry with an even number of poles be a valid coupled fluxes device?

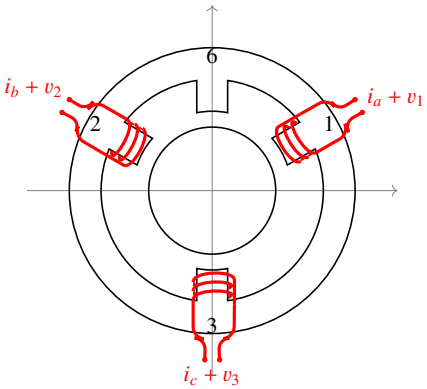

Fig. 5 Type C: a symmetry of 3 device with an even number of poles.

The ferromagnetic connections in type C allow a current in any winding to cause fluxes in all air gaps. If ϕ_{jk} denotes the flux in air gap j caused by a current in winding k, and assuming no losses and positive signs for fluxes headed to the center, the magnetic fluxes at the poles are:

$$\phi_1 = \phi_{11} - \phi_{12} - \phi_{13}, \quad \phi_2 = -\phi_{21} + \phi_{22} - \phi_{23}, \quad \phi_3 = -\phi_{31} - \phi_{32} + \phi_{33}, \quad \phi_6 = -\phi_{61} - \phi_{62} - \phi_{63}. \tag{19}$$

The forces in channels $k = 1, 2, 3$ are given by equation (2). The circuit in figure 6 models a situation when pole 1 is generating flux; the magneto-motive force due to i_1 is $\mathcal{F}_1$ and the gaps reluctances are $\mathcal{R}_1$, $\mathcal{R}_2$, $\mathcal{R}_3$ and $\mathcal{R}_6$. Magnetic circuits can be studied with the passive electric circuit analogy: reluctance $\mathcal{R}_1$ in the figure is in series with the parallel combination of $\mathcal{R}_2$ $\mathcal{R}_3$ and $\mathcal{R}_6$. A careful analysis of this diagram would result in expressions for the $\phi_{k1}, k = 1, 2, 3, 6$.

Repeating this procedure for the other windings allows the determination of the ϕ_{ij}; the long details are not shown here. To understand the final results consider the auxiliary variables depending on the displacements d_k and on the injected i_k, which must be defined in a very general way, with different values for the base currents: $i_1 = i_a + v_1$, $i_2 = i_b + v_2$ and $i_3 = i_c + v_3$.

$$D_{ij} = d_i d_j, \quad D_{ijk} = d_i d_j d_k, \quad \Delta = D_{123} + D_{126} + D_{136} + D_{236} \tag{20}$$

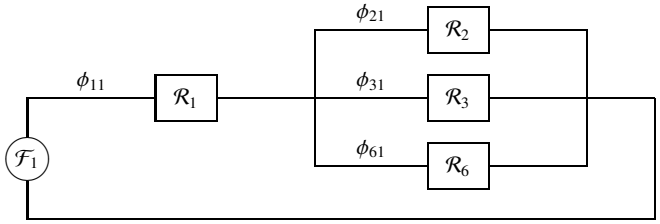

Fig. 6 Magnetic flux equivalent circuit associated with current $i_1(t)$.

$$N_1 = D_{23}(i_a + v_1) + D_{26}(i_a - i_c + v_1 - v_3) + D_{36}(i_a - i_b + v_1 - v_2), \tag{21}$$

$$N_2 = D_{13}(i_b + v_2) + D_{16}(i_b - i_c + v_2 - v_3) + D_{36}(i_b - i_a + v_2 - v_1), \tag{22}$$

$$N_3 = D_{12}(i_c + v_3) + D_{16}(i_c - i_b + v_3 - v_2) + D_{26}(i_c - i_a + v_3 - v_1), \tag{23}$$

$$N_6 = -D_{23}(i_a + v_1) - D_{13}(i_b + v_2) - D_{12}(i_c + v_3). \tag{24}$$

The fluxes ϕ_k can be determined: $\phi_1 = \mu_0 AnN_1/\Delta$, $\phi_2 = \mu_0 AnN_2/\Delta$, $\phi_3 = \mu_0 AnN_3\Delta$, $\phi_6 = -\mu_0 AnN_6/\Delta$ and, using (2), the forces in the three channels can be expressed as: $F_1 = \mu_0 An^2 N_1^2/\Delta^2$, $F_2 = \mu_0 An^2 N_2^2/\Delta^2$, $F_3 = \mu_0 An^2(N_3^2 - N_6^2)/\Delta^2$. The resultant forces in the x and y directions can be found, once again, with the help of equation (1), recalling that $K_0 = \mu_0 An^2$:

$$f_x = K_0\sqrt{3}\frac{\left(N_1^2 - N_2^2\right)}{2\Delta^2} \qquad \text{and} \qquad f_y = K_0\frac{\left(N_1^2 + N_2^2 - 2(N_3^2 - N_6^2)\right)}{2\Delta^2}. \tag{25}$$

Using (8) in the previous expression leads to $f_{xy} = g_{xy}(x, y, v_1, v_2, v_3)$. A linearization around the operating point OP $= (x^o, y^o, v_1^o, v_2^o, v_3^o) = (0, 0, 0, 0, 0)$ is characterized by

$$f_x - [f_x]_o = \sum_{k=1}^{3}\left[\frac{\partial f}{\partial v_k}\right]_o (v_k - v_k^o) + \left[\frac{\partial f}{\partial x}\right]_o (x - x^o) + \left[\frac{\partial f}{\partial y}\right]_o (y - y^o) \tag{26}$$

$$f_y - \left[f_y\right]_o = \sum_{k=1}^{3}\left[\frac{\partial g}{\partial v_k}\right]_o (v_k - v_k^o) + \left[\frac{\partial g}{\partial x}\right]_o (x - x^o) + \left[\frac{\partial g}{\partial y}\right]_o (y - y^o) \tag{27}$$

The values of f_{xy} at the operating point can be shown to be $[f_x]_o = K_0\sqrt{3}(i_a + i_b - i_c)(i_a - i_b)/(4h^2)$ and $\left[f_y\right]_o = K_0(5i_a^2 + 5i_b^2 - 7i_c^2 + 6i_a i_c + 6i_b i_c - 6i_a i_b)/(16h^2)$. A simple calculation shows the existence of two possible solutions that make both these values 0, as they should: solution I is $i_a = i_b = i_0, i_c = 2i_0$ and solution II is $i_a = i_b = i_0, i_c = -2i_0/7$. Solution I leads to $[N_1]_0 = [N_2]_0 = 0$, $[N_3]_0 = 4h^2 i_0$ and $[N_6]_0 = -4h^2 i_0$. Making $K_0\sqrt{3}/(2\Delta^2) = K$ in (26) the partial derivative of $f_x = KN_1^2 - KN_2^2$ can be found:

$$\frac{\partial f_x}{\partial v_k} = \frac{\partial f_x}{\partial N_1}\frac{\partial N_1}{\partial v_k} + \frac{\partial f_x}{\partial N_2}\frac{\partial N_2}{\partial v_k} = 2KN_1\frac{\partial N_1}{\partial v_k} - 2KN_2\frac{\partial N_2}{\partial v_k}. \tag{28}$$

Since $[N_1]_0 = [N_2]_0 = 0$ this derivative evaluated at the OP is zero and no linearization can be made. Again. But Solution II gives another solution $i_a = i_b = i_0$, $i_c = -2i_0/7$ and with this choice the N_i values at the operating point are $[N_1]_0 = 16h^2 i_0/7, [N_2]_0 = 16h^2 i_0/7, [N_3]_0 = -20h^2 i_0/7, [N_6]_0 = -12h^2 i_0/7$ and the partial derivatives are

$$\left[\frac{\partial f_x}{\partial v_1}\right]_o = \frac{4\sqrt{3}K_0 i_0}{7h^2}, \qquad \left[\frac{\partial f_x}{\partial v_2}\right]_o = -\frac{4\sqrt{3}K_0 i_0}{7h^2}, \qquad \left[\frac{\partial f_x}{\partial v_3}\right]_o = 0 \tag{29}$$

where $K_0 = \mu_0 An^2$. The expression for f_x in the left side of (25) leads to

$$\frac{\partial f_x}{\partial x} = \frac{\partial f_x}{\partial N_1}\frac{\partial N_1}{\partial x} + \frac{\partial f_x}{\partial N_2}\frac{\partial N_2}{\partial x} + \frac{\partial f_x}{\partial \Delta}\frac{\partial \Delta}{\partial x} \quad \text{and} \quad \frac{\partial f_x}{\partial y} = \frac{\partial f_x}{\partial N_1}\frac{\partial N_1}{\partial y} + \frac{\partial f_x}{\partial N_2}\frac{\partial N_2}{\partial y} + \frac{\partial f_x}{\partial \Delta}\frac{\partial \Delta}{\partial y}. \tag{30}$$

A careful calculation of the partial derivatives above is a long and cumbersome endeavour and its details will not be shown here; the final result is

$$\left[\frac{\partial f_x}{\partial x}\right]_o = \frac{48K_0 i_0^2}{49h^3} \qquad \text{and} \qquad \left[\frac{\partial f_x}{\partial y}\right]_o = 0. \tag{31}$$

The same procedure should be applied to f_y in (25); it is a longer and cumbersome task and the readers will be, once again, spared of the details. The final results are

$$\left[\frac{\partial f_y}{\partial x}\right]_o = 0, \qquad \left[\frac{\partial f_y}{\partial y}\right]_o = \frac{66K_0i_0^2}{49h^3}, \qquad \left[\frac{\partial f_y}{\partial v_1}\right]_o = \frac{K_0i_0}{7h^2}, \qquad \left[\frac{\partial f_y}{\partial v_2}\right]_o = \frac{K_0i_0}{7h^2}, \qquad \left[\frac{\partial f_y}{\partial v_3}\right]_o = \frac{K_0i_0}{h^2}. \tag{32}$$

Based on (26) and (27) a first version of the linearized model, using he differential currents v_k, can be written:

$$f_x = \frac{48K_0i_0^2}{49h^3}x + \frac{4\sqrt{3}K_0i_0}{7h^2}(v_1 - v_2) \qquad \text{and} \qquad f_y = \frac{66K_0i_0^2}{49h^3}y + \frac{K_0i_0}{7h^2}(v_1 + v_2 + 7v_3). \tag{33}$$

One possible way to express the v_k in terms of only two variables i_x and i_y is by choosing $v_1 = \sqrt{3}i_x/2 + i_y, v_2 = \sqrt{3}i_x/4 + i_y, v_3 = -3\sqrt{3}i_x/28 + i_y/7$. After this, the linearized model can be finally given by

$$f_x = 8k_px + k_ii_x \quad \text{and} \quad f_y = 6k_py + k_ii_y \quad \text{where} \quad k_p = \frac{6K_0i_0^2}{49h_3} \quad \text{and} \quad k_i = \frac{3K_0i_0}{7h^2}. \tag{34}$$

Even though the position constants for x and y are not the same a decoupled structure appears, and this is a very welcome fact. A Sym3 device that can be linearized was found at last, after a long and unsuccessful search.

With the same conditions used previously for the LQR control, this device was simulated in Openmodelica; the side figure shows the curves x (red) and y (green), obtained from the complete, non-linear equations, and also x_l (red) and y_l (violet) from the linearized model. The performance is as fast as before, reaching the steady state in about 0.16s, but the curves x and y show a little overshoot. In the previous case, the non-linear (x, y) and the linear (x_l, y_l) curves were almost completely coincident, but now a noticeable difference exists between them.

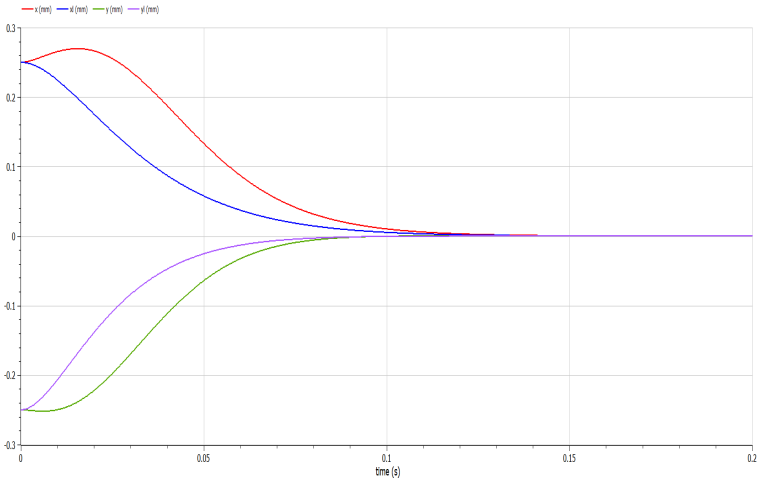

5. Conclusions

In the Sym4 world CF devices work as good as UF ones. It was expected that the same would happen in Sym3 with 06 and 03 poles, but a lot of CF cases have been studied with disappointing results because of linearization issues. It appeared that this geometry could not exist in the real world. The Type C case shown in section 4 proved that Sym3 CF structures can exist, and this is a good thing, but are they good? can they be compared to Sym3 and Sym4 UF?

The last simulations show that Type C performance is as fast as in the cases in section 3, but with a small overshoot. A remarkable fact is the non-negligible difference between the displacements obtained from the real and linearized models. These curves were practically the same in the previous simulations for Sym4 and Sym3 UF devices. This is a sound evidence that the linearization problems found so many times in Sym3 UF devices are something that deserves more research, if the idea of having Sym3 CF devices working in real-life applications is considered seriously.

6. Acknowledgements

The authors are very happy to express their deep gratitude to Prof. Richard Magalena Stephan for his continuous presence, friendship, and solid technical bits of advice.

7. References

[1] D. D. F. Brito and A. C. D. N. Gomes. Comparing magnetic bearings with symmetry of 3. In Proceedings of ISMB18, 18th International Symposium on Magnetic Bearings, http://www.magneticbearings.org/publications, 2023.

[2] S. Chen and C. Hsu. Optimal design of a three-pole active magnetic bearing. IEEE Transactions on Magnetics, 38:3458–3466, September 2002.
[3] A. Chiba, T. Fukao, O. Ichikawa, M. Oshima, M. Takemoto, and D. Dorrell. Magnetic Bearings and Bearingless Drives. Newnes-Elsevier, 2005.
[4] D. F. B. David, J. A. Santisteban, and A. C. Del Nero Gomes. Interconnected four poles magnetic bearings. In Proceedings of the 1st Brazilian Workshop on Magnetic Bearings, www.magneticbearings2103.com.br, october 2013.
[5] D. F. B. David, J. A. Santisteban, and A. C. Del Nero Gomes. Interconnected four poles magnetic bearings simulations and testing. In Proceedings of ISMB14, 14th International Symposium on Magnetic Bearings, pages 30–35, http://ismb14.magneticbearings.org, august 2014.
[6] D. F. B. David, J. A. Santisteban, and A. C. Del Nero Gomes. Laboratory tests on an interconnected four poles magnetic bearing. In Proceedings of ISMB15, 15th International Symposium on Magnetic Bearings, august 2016.
[7] D. F. B. David, J. A. Santisteban, and A. C. Del Nero Gomes. Modeling and testing strategies for an interconnected four-pole magnetic bearing. Actuators, 6(21), 2017.
[8] N. R. Hemenway and E. L.Severson. Three-pole magnetic bearing design and actuation. IEEE Transactions on Industry Applications, 56(Issue: 6):6348–6359, 2020. https://ieeexplore.ieee.org/document/9154570.
[9] Laura J. M. Mothé, Vinicius R. Vasco, Y. P. Corrêa, D. D. F. Brito, and A. C. D. N. Gomes. Model and control of a six-pole magnetic bearing. In Proceedings of ISMB17, 17th International Symposium on Magnetic Bearings, http://www.magneticbearings.org/publications, 2021.
[10] G. Schweitzer, H. Bleuler, and A. Traxler. Active Magnetic Bearings. Hochshulverlag AG an der ETH Zürich, 1994.
[11] G. Schweitzer, E. Maslen, H. Bleuler, M. Cole, P. Keogh, R. Larsonneur, R. Nordmann, and Y. Ogada. Magnetic Bearings: Theory, Design and Applications to Rotating Machinery. Springer-Verlag, 2009.
[12] W. Zhang and H. Zhu. Radial magnetic bearings: an overview. Results in Physics, 7:3756–3766, 2017.